

# Nox2-derived oxidative stress results in inefficacy of antibiotics against post-influenza *S. aureus* pneumonia

Keer Sun,<sup>1,2</sup> Vijaya Kumar Yajjala,<sup>1</sup> Christopher Bauer,<sup>1</sup> Geoffrey A. Talmon,<sup>1</sup> Karl J. Fischer,<sup>1</sup> Tammy Kielian,<sup>1</sup> and Dennis W. Metzger<sup>2</sup>

<sup>1</sup>Department of Pathology and Microbiology, University of Nebraska Medical Center, Omaha, NE 68198

<sup>2</sup>Center for Immunology and Microbial Disease, Albany Medical College, Albany, NY 12208

**Clinical post-influenza *Staphylococcus aureus* pneumonia is characterized by extensive lung inflammation associated with severe morbidity and mortality even after appropriate antibiotic treatment. In this study, we show that antibiotics rescue nicotinamide adenine dinucleotide phosphate (NADPH) oxidase 2 (Nox2)-deficient mice but fail to fully protect WT animals from influenza and *S. aureus* coinfection. Further experiments indicate that the inefficacy of antibiotics against coinfection is attributable to oxidative stress-associated inflammatory lung injury. However, Nox2-induced lung damage during coinfection was not associated with aggravated inflammatory cytokine response or cell infiltration but rather caused by reduced survival of myeloid cells. Specifically, oxidative stress increased necrotic death of inflammatory cells, thereby resulting in lethal damage to surrounding tissue. Collectively, our results demonstrate that influenza infection disrupts the delicate balance between Nox2-dependent antibacterial immunity and inflammation. This disruption leads to not only increased susceptibility to *S. aureus* infection, but also extensive lung damage. Importantly, we show that combination treatment of antibiotic and NADPH oxidase inhibitor significantly improved animal survival from coinfection. These findings suggest that treatment strategies that target both bacteria and oxidative stress will significantly benefit patients with influenza-complicated *S. aureus* pneumonia.**

## INTRODUCTION

During recent influenza pandemics and epidemics, post-influenza methicillin-resistant *Staphylococcus aureus* (MRSA) infection has emerged as a leading contributor to death (Metzger and Sun, 2013). It is well recognized that influenza infection inhibits antibacterial immunity, thereby increasing susceptibility to secondary bacterial infection (Small et al., 2010; Kudva et al., 2011; Robinson et al., 2013). However, even with appropriate antibiotic treatment, the mortality rate of patients with post-influenza MRSA pneumonia remains >50% (Vardakas et al., 2009). The inefficacy of antibiotic therapy has led to the assumption that defective bacterial control is not the only determinant of disease severity. However, the incomplete understanding of pathogenic mechanisms has hindered the development of effective treatments against influenza and MRSA coinfection (Vardakas et al., 2009; Meter-sky et al., 2012; Blyth et al., 2013).

Nicotinamide adenine dinucleotide phosphate (NADPH) oxidase 2 (Nox2), also known as gp91phox, is the catalytic subunit of NADPH oxidase in phagocytes. In humans, defects in X chromosome-linked Nox2 can lead to chronic granulomatous disease (CGD). Activation of Nox2, a process

called oxidative burst, is critical for immune defense against *S. aureus* infection (Sun and Metzger, 2014). In contrast, as a result of the nonspecific action of reactive oxygen species (ROS), Nox2 is known to be involved in inflammatory tissue damage (Imai et al., 2008; von Dessauer et al., 2011), including acute lung injury during influenza infection (Akaike et al., 1996; Snelgrove et al., 2006; Imai et al., 2008; Vlahos et al., 2011). We have recently demonstrated that intracellular ROS levels in phagocytes decrease after influenza infection. This decrease leads to defective bacterial killing and susceptibility to secondary *S. aureus* infection (Sun and Metzger, 2014). Furthermore, we hypothesize that during influenza and *S. aureus* coinfection, in addition to defective antibacterial immunity, a concomitant but contrasting contribution of oxidative burst to acute lung injury leads to immune dysregulation and, consequently, poor disease outcomes.

Over half of the cases of patients with *S. aureus* necrotizing pneumonia are fatal even after administration of appropriate antibiotics (Vardakas et al., 2009). Death from influenza and/or bacterial pneumonia is generally associated with the development of acute respiratory distress syndrome (ARDS), a condition characterized by extensive inflammatory injury to the alveolar capillary barrier (Matute-Bello et al., 2008; Short et al., 2014; Han and Mallampalli, 2015). De-

Correspondence to Keer Sun: Keer.sun@unmc.edu

Abbreviations used: ARDS, acute respiratory distress syndrome; BAL, bronchoalveolar lavage; BALF, BAL fluid; CGD, chronic granulomatous disease; dpi, days postinfection; FVD, fixable viability dye; LDH, lactate dehydrogenase; MPO, myeloperoxidase; MRSA, methicillin-resistant *Staphylococcus aureus*; NADPH, nicotinamide adenine dinucleotide phosphate; Nox2, NADPH oxidase 2; ROS, reactive oxygen species.

© 2016 Sun et al. This article is distributed under the terms of an Attribution-Noncommercial-Share Alike-No Mirror Sites license for the first six months after the publication date (see <http://www.rupress.org/terms>). After six months it is available under a Creative Commons License (Attribution-Noncommercial-Share Alike 3.0 Unported license, as described at <http://creativecommons.org/licenses/by-nc-sa/3.0/>).

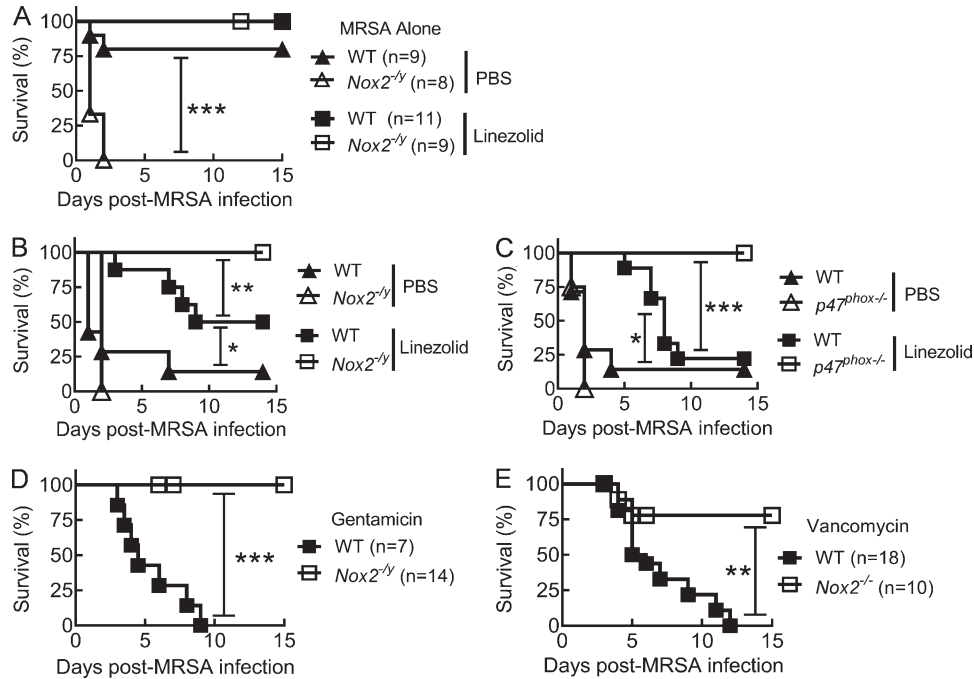


**Figure 1. NADPH oxidase activity and antibiotic inefficacy against coinfection.** (A) Survival of C57BL/6 WT and *Nox2*<sup>-/-</sup> mice infected with MRSA only. Infected mice were treated daily with the linezolid or PBS. (B–E) Survival of C57BL/6 WT (7–10 mice/group), *Nox2*<sup>-/-</sup> (7–10 mice/group), *p47<sup>phox</sup>*<sup>-/-</sup> mice (8–10 mice/group), and *Nox2*<sup>-/-</sup> mice superchallenged with MRSA on day 7 after PR8 virus infection. Coinfected mice were treated daily with the antibiotics linezolid (B and C), gentamicin (D), or vancomycin (E). In B and C, control mice were treated daily with PBS. \*, *P* < 0.05; \*\*, *P* < 0.01; \*\*\*, *P* < 0.001, log-rank test. Data shown in A were combined from two independent experiments. Data shown in B–E are representative of at least two independent experiments.

spite improved supportive care, there is currently no specific treatment for inflammatory lung damage that is based on a known molecular pathway.

In the present study, we examined whether the inefficacy of antibiotics against post-influenza *S. aureus* infection is caused by *Nox2*-derived, ROS-mediated inflammatory lung damage. Indeed, we found that antibiotic inhibition of bacterial outgrowth provided complete protection against influenza and MRSA coinfection only in the absence of oxidative burst. However, we found that the adverse role of *Nox2* was not caused by aggravated inflammatory cytokine production or cell accumulation, but rather, it was caused by reduced survival of myeloid cells. Furthermore, in contrast to the cell-intrinsic contribution of ROS to phagocytic bacterial killing (Sun and Metzger, 2014), our studies in *Nox2*<sup>+/-</sup> mosaic mice (i.e., female carriers of X-linked *Nox2* deficiency) revealed that *Nox2*-driven oxidative stress accelerated necrotic cell death and caused direct lung damage.

## RESULTS

### Detrimental role of *Nox2* during influenza and MRSA coinfection

To mimic clinical events in which influenza infection predisposes individuals to *S. aureus* infection, we challenged NADPH oxidase-deficient and WT mice with a sublethal dose of PR8 influenza virus followed by i.n. superinfection with

MRSA 7 d later (Sun and Metzger, 2014). In agreement with previous studies (Köhler et al., 2011; Sun and Metzger, 2014), *Nox2*-deficient mice were more susceptible to *S. aureus* infection alone; however, in the absence of influenza infection, daily treatment with the bacteriostatic antibiotic linezolid was sufficient to protect both WT and *Nox2*<sup>-/-</sup> males (Fig. 1 A). Conversely, without antibiotic treatment, nearly all influenza-infected WT and *Nox2*<sup>-/-</sup> mice succumbed to subsequent MRSA infection (Fig. 1 B). WT mice treated daily with the antibiotic linezolid exhibited extended survival times compared with PBS-treated controls, but >50% of them eventually succumbed to post-influenza MRSA infection. In contrast, all linezolid-treated *Nox2*<sup>-/-</sup> (Fig. 1 B) mice survived influenza and MRSA coinfection.

*P47<sup>phox</sup>* is the cytosolic subunit of NADPH oxidase and is required for enzyme activation and subsequent superoxide production (Abo et al., 1992). Similar to *Nox2*-deficient mice, linezolid treatment protected all *p47<sup>phox</sup>*<sup>-/-</sup> mice from an otherwise lethal coinfection (Fig. 1 C). Furthermore, daily treatment of the antibiotic gentamicin (Fig. 1 D) or vancomycin (Fig. 1 E) rescued *Nox2*-deficient mice but failed to protect WT animals from lethal coinfection (Fig. 1, D and E). Of note, at equivalent inoculating doses, neither influenza (not depicted) nor MRSA infection alone (Fig. 1 A) caused death in linezolid-treated WT or *Nox2*-deficient controls. These striking differences in the efficacy of antibiotic

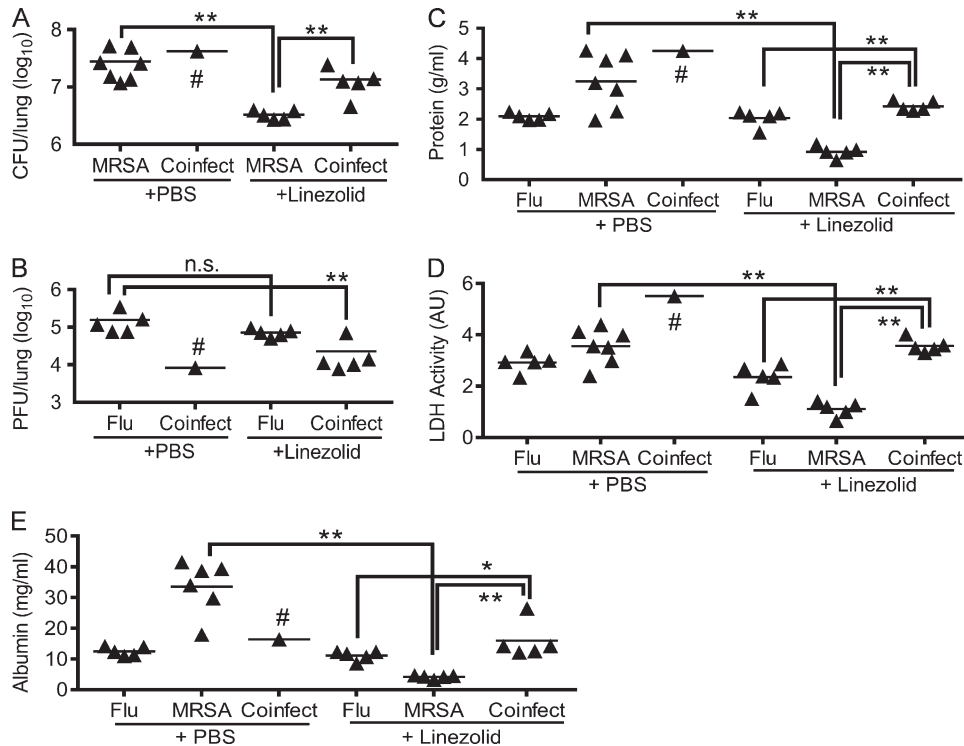


Figure 2. **Antibiotic treatment controls lung bacterial burdens.** (A–E) WT mice were infected with PR8 and 7 d later superchallenged with MRSA. At 1 dpi, lungs were analyzed for bacterial burdens (A), viral titers (B), protein (C), LDH (D), and albumin levels (E) in BALF. All PR8-infected (Flu), MRSA-infected (MRSA), and coinfect (Flu + MRSA) mice were treated with linezolid or PBS control. #, four out of five coinfect mice died within 24 h in the absence of linezolid treatment; AU, arbitrary units; n.s., not significant. \*,  $P < 0.05$ ; \*\*,  $P < 0.01$ , Mann Whitney test. Data shown are representative of two independent experiments.

treatment between Nox2-deficient and WT mice implicate a detrimental role of oxidase burst during post-influenza *S. aureus* infection, which is usually masked by its protective antibacterial function.

### Nox2 exacerbates lung damage during influenza and MRSA coinfection

We next investigated the therapeutic effect of antibiotics during influenza and/or MRSA infection. As expected, antibiotic treatment reduced bacterial burdens during MRSA infection but did not appear to have a significant effect on viral titers after influenza infection alone (Fig. 2, A and B). Conversely, antibiotic treatment was essential for prolonged animal survival after coinfection. Interestingly, compared with PR8-infected and PBS-treated controls, coinfect and antibiotic-treated WT mice exhibited temporary decreases in detectable viral titers, probably because of the combined stimulatory effects of MRSA superinfection and linezolid treatment (Fig. 2 B). Albumin efflux as well as protein and lactate dehydrogenase (LDH) levels in airway fluids were next assessed as indications of lung vascular and tissue damage. In agreement with the bacterial control, linezolid treatment greatly attenuated lung tissue damage during MRSA infection alone. Nonetheless, compared with either influenza or

MRSA infection alone, acute lung injury was significantly aggravated after influenza and MRSA coinfection, even after antibiotic treatment (Fig. 2, C–E).

To determine how Nox2 activity renders antibiotic therapy ineffective against influenza and MRSA coinfection, we next investigated the possible negative impact of oxidative burst on the bactericidal activity of the antibiotic linezolid (Kohanski et al., 2010; Liu and Imlay, 2013). Conversely, we found that during the course of infection, bacterial burdens were persistently higher in coinfect Nox2-deficient mice compared with WT animals (Fig. 3 A). We have previously reported that influenza infection suppresses NADPH oxidase-dependent phagocytic bacterial clearance (Sun and Metzger, 2014). Indeed, in contrast to WT mice, Nox2-deficient mice showed similar increased bacterial burdens at 1 d postinfection (dpi) after either MRSA infection alone or coinfection (Fig. 3 A). Notably, Nox2 has been reported to delay viral clearance during influenza infection alone (Vlahos et al., 2011). However, viral burdens were similar in influenza-infected WT and Nox2-deficient mice after inoculation of MRSA or PBS control (Fig. 3 B), suggesting that neither Nox2 activity nor MRSA superinfection significantly suppresses viral clearance. Moreover, both viral and bacterial burdens in the lungs declined when coinfect WT mice suc-

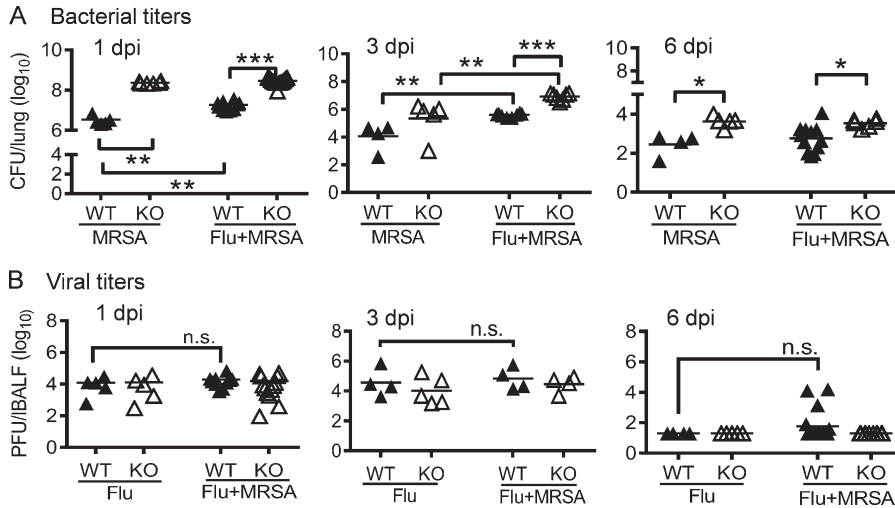


**Figure 3. Nox2 activity enhances lung bacterial clearance.** (A and B) WT and Nox2-deficient (KO) mice were infected with PR8 and 7 d later superchallenged with MRSA. Lungs were analyzed for bacterial burdens (A) and viral titers (B). All PR8-infected (Flu), MRSA-infected (MRSA), or coinfecting (Flu + MRSA) mice were treated daily with linezolid until 24 h before harvesting the samples. \*,  $P < 0.05$ ; \*\*,  $P < 0.01$ ; \*\*\*,  $P < 0.001$ , Tukey's multiple comparisons test. n.s., not significant. Data shown are representative of two independent experiments.

cumbed to disease (Figs. 1 and 3). Of note, in this particular study, all animals received antibiotic treatment, including mice infected with influenza virus or MRSA alone (Fig. 3). Together, these results establish that the lethal contribution of Nox2 to the outcome of coinfection is not caused by its influence on viral clearance or the bactericidal effect of antibiotics, but instead, it is likely caused by the undue damage inflicted by the inflammatory responses of the host.

Extreme inflammatory lung damage is indeed a characteristic feature of *S. aureus* pneumonia, as consistently demonstrated in both humans and animal models (Louria et al., 1959; Centers for Disease Control and Prevention (CDC), 2007; Small et al., 2010; Iverson et al., 2011; Kudva et al., 2011). Additionally, multiple studies establish that ROS produced by phagocytes can cause inflammatory diseases (Imai et al., 2008; Vlahos et al., 2011). Considering that Nox2 is responsible for inducible ROS production in phagocytes, we sought to determine whether lethal coinfection in WT animals is associated with Nox2-induced inflammatory lung damage. At early time points of infections, we did not observe attenuation of lung damage in Nox2-deficient mice as compared with corresponding WT controls (Fig. 4, A and B). However, coinfecting WT mice did exhibit a significant delay in resolution of inflammation, as revealed by elevated levels of albumin and LDH in airways at 6 dpi (Fig. 4 C). Notably, at this later time point, there were no detectable viral titers in either WT or Nox2-deficient mice infected with PR8 only (Fig. 3 B). Conversely, despite their residual bacterial burdens at 6 dpi (Fig. 3 A), inflammatory lung damage was not evident in WT and Nox2-deficient mice inoculated with MRSA only (Fig. 4 C). Such observations suggest that after appropriate antibiotic treatment for coinfection, Nox2-induced lung injury, rather than viral or bacterial outgrowth, is the fundamental determinant of disease outcome.

To characterize Nox2-induced inflammatory lung damage, we evaluated the lung histopathology of antibiotic-treated Nox2-deficient and WT mice at 6 dpi (Fig. 4 D).

The majority of WT mice exhibited extensive lung damage accompanied by prominent intraalveolar protein and/or fibrin extravasation, a characteristic feature of ARDS. Further, the degree of parenchymal damage significantly increased in the lungs of WT mice compared with Nox2-deficient animals (Fig. 4 E). Conversely, although proinflammatory cytokine production was significantly enhanced after MRSA superinfection, their levels were comparable in coinfecting WT and Nox2-deficient mice (Fig. 5, A–E). In fact, Nox2-deficient mice demonstrated significantly increased IL-17 production early (1 dpi) after MRSA infection (Fig. 5 D). Nonetheless, airway inflammatory cytokine production was essentially diminished in both WT and Nox2-deficient mice at the later stage of coinfection (Fig. 5). Collectively, these results indicate that during influenza and MRSA coinfection, as distinct from influenza infection alone (Akaike et al., 1996; Snelgrove et al., 2006; Imai et al., 2008; Vlahos et al., 2011), Nox2-induced lung injury does not correlate with an aggravated cytokine response at the site of infection.

#### Nox2 activity during coinfection reduces myeloid cell survival

We next determined whether Nox2-induced lung injury correlates with extensive inflammatory cell infiltration. As expected, neutrophil influx was greatly enhanced after MRSA superinfection (Fig. 6 A). Interestingly, compared with WT mice, coinfecting Nox2-deficient mice demonstrated further increases in accumulation of neutrophils at 1 dpi (Fig. 6 A). Even so, this effect is transient, considering that neutrophil numbers dramatically declined in both WT and Nox2-deficient mice at 6 dpi (Fig. 6, B and C). In addition, the relative numbers of CD11c<sup>+</sup> resident alveolar macrophages and inflammatory monocytes were also comparable in coinfecting WT and Nox2-deficient mice at 6 dpi (Fig. 6, D and E).

Notably, inflammatory cells are short lived, and their numbers at a given time point are the result of simultaneous recruitment and removal (Bratton and Henson, 2011; Geer-

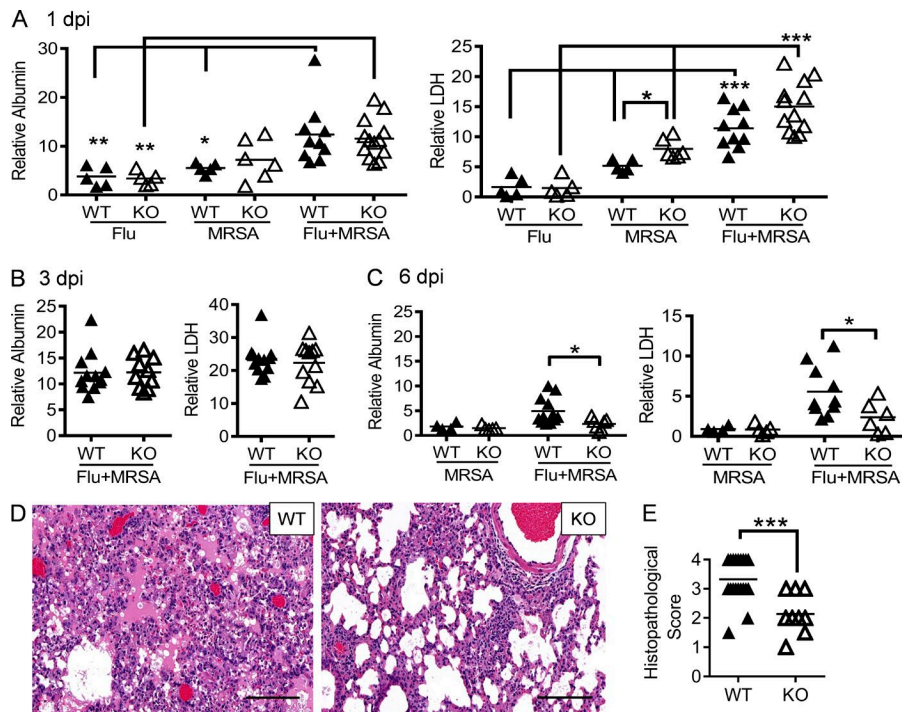


**Figure 4. Nox2 activity during coinfection exacerbates tissue damage.** (A–C) WT and Nox2-deficient (KO) mice were infected with PR8 and 7 d later superchallenged with MRSA. BALFs were analyzed for albumin and LDH levels at days 1 (A), 3 (B), and 6 (C) after infection. Data represent albumin and LDH levels relative to these in naive WT mice. \*,  $P < 0.05$ ; \*\*,  $P < 0.01$ ; \*\*\*,  $P < 0.001$ , Tukey's multiple comparisons test. (D and E) At 6 dpi, lungs were analyzed for histopathology (H&E; D) and histopathologic scores (each symbol represents one mouse; E). (E) Whole mount H&E-stained sections of lung tissue from each mouse were semiquantitatively assessed at low power (100 $\times$ ) for the proportion of parenchyma with alveoli-containing intraluminal material (proteinaceous exudate and/or fibrin) in the background of interstitial expansion and inflammation. Each lung was scored by the relative amount of abnormal tissue as follows: normal = 0; 1–25% = 1; 26–50% = 2; 51–75% = 3; >76% = 4. \*\*\*,  $P < 0.001$ , Student's *t* test. Bars, 100  $\mu$ m. All PR8-infected (Flu), MRSA-infected (MRSA), or coinfecting mice (Flu + MRSA) were treated daily with linezolid until 24 h before harvesting the samples. Data shown in (A–D) are representative of two independent experiments. Data shown in E were combined from two independent experiments.

ing and Simon, 2011; Janssen et al., 2011). Interestingly, we found that CD11b<sup>+</sup> myeloid cells from WT mice at 1 dpi exhibited a significant reduction in survival time, as indicated by increases in both early apoptotic (annexin<sup>+</sup>fixable viability dye [FVD]<sup>low</sup>) and late apoptotic/necrotic (annexin<sup>+</sup>FVD<sup>hi</sup>) cells (Fig. 7, A and B). By 3 dpi, over half of the WT inflammatory cells in the airways became apoptotic or necrotic (Fig. 7 C). The proportions of dying CD11b<sup>+</sup> inflammatory cells significantly increased in WT airways at 6 dpi, which was followed by overt cell necrosis (Fig. 7 D). Together, these results indicate that rather than regulating inflammatory infiltration, Nox2 activity accelerates inflammatory cell death during post-influenza MRSA infection.

### Nox2-derived extracellular ROS accelerate necrotic cell death

Considering 100-fold decreases in neutrophil numbers within 3 d in both coinfecting WT and Nox2-deficient mice (Fig. 6, B and C), the detectable levels of dying cells in vivo were relatively infrequent (Fig. 7 D). This is likely because of macrophage-mediated efferocytosis of apoptotic cells or disintegration of necrotic cells. Conversely, the proportions of late apoptotic/necrotic WT inflammatory cells were significantly increased after 24 h in culture (Fig. 7, E–G), despite treatment with the necrosis inhibitor IM-54 (Sodeoka and Dodo, 2010) or necroptosis inhibitor necrostatin 1 (Su et al., 2015). These

observations imply that Nox2 activity may promote not only inflammatory cell apoptosis, but also their progress to autolytic secondary necrosis after coinfection.

Of note, the Nox2 subunit is an X chromosome-linked gene. Female Nox2<sup>+/-</sup> (mosaic) mice contain both WT (Nox2<sup>+</sup>) and Nox2-deficient (Nox2<sup>-</sup>) neutrophils because of random inactivation of the X chromosome in individual cells (Sun and Metzger, 2014). Therefore, to investigate the contribution of oxidative burst to neutrophil survival in vivo, we examine the frequency of Nox2-positive and Nox2-deficient neutrophils in mosaic mice before and after infections. If the oxidative burst process in activated neutrophils compromises their own survival, we expected decreased proportions of Nox2<sup>+</sup> neutrophils in mosaic mice at the site of infection (Sun and Metzger, 2014). On the contrary, we found that during the course of infection, the ratio of Nox2<sup>+</sup> and Nox2<sup>-</sup> neutrophils remained essentially the same in the blood (Fig. 8, A and B) and airways (Fig. 8, A and C). These observations indicate that despite their cell-intrinsic defect in oxidative burst, Nox2-deficient neutrophils have a similar lifespan as WT neutrophils in the same environment. Furthermore, this suggests that the regulatory effect of Nox2-derived ROS on neutrophil survival is not cell intrinsic during influenza and/or MRSA infections.

The findings in the previous paragraph imply that extracellular ROS levels are responsible for neutrophil turnover

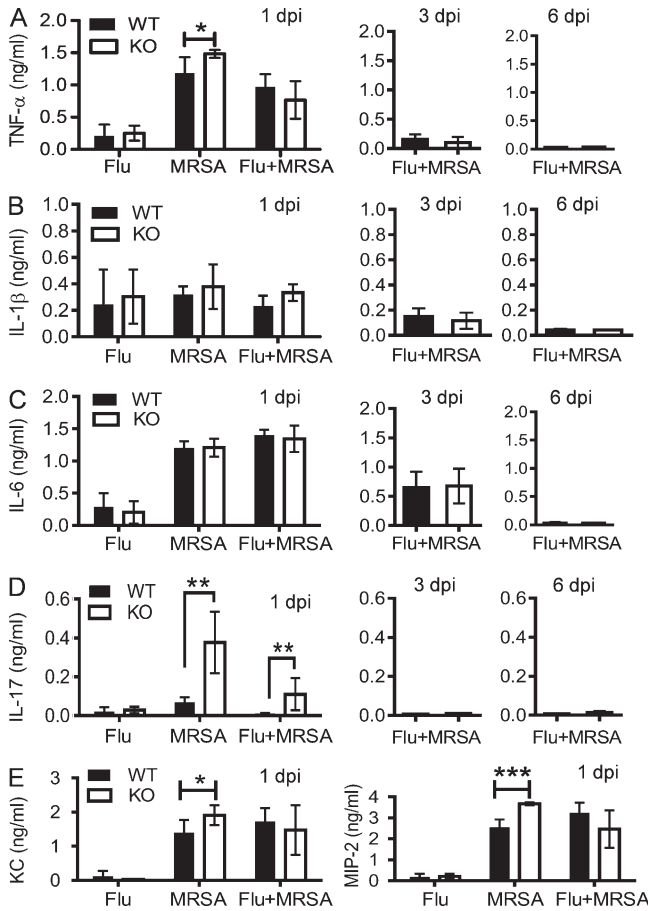


**Figure 5. Nox2 activity during coinfection does not enhance inflammatory cytokine response.** (A–E) WT and Nox2-deficient (KO) mice were infected with PR8 and 7 d later superchallenged with MRSA. BALFs were analyzed for TNF- $\alpha$  (A), IL-1 $\beta$  (B), IL-6 (C), IL-17 (D), and keratinocyte-derived chemokine and MIP-2 (E) levels at days 1, 3, and 6 after infection. All PR8-infected (Flu), MRSA-infected (MRSA), or coinfecting (Flu + MRSA) mice ( $n \geq 4$ ) were treated daily with linezolid until 24 h before harvesting the samples. \*,  $P < 0.05$ ; \*\*,  $P < 0.01$ ; \*\*\*,  $P < 0.001$ , Student's  $t$  test. Data shown are representative of two independent experiments and are means  $\pm$  SD.

rates in mice. We next investigated whether, similar to WT females, this Nox2-dependent, accelerated inflammatory cell death also occurred in coinfecting  $Nox2^{+/-}$  mosaic mice. Interestingly, mosaic mice showed similar proportions of apoptotic neutrophils compared with  $Nox2^{-/-}$  females (Fig. 8, D and E); however, similar to WT controls, the percentage of necrotic cells significantly increased in the airways of mosaic mice (Fig. 8, D and E). These results indicate that extracellular ROS levels are indeed responsible for increased necrotic cell death during influenza and MRSA coinfection.

**Systemic oxidative stress induces lethal inflammation during coinfection**

Excessive release of toxic products from necrotic cells has long been known to cause tissue damage and subsequent organ fail-

ure. To determine whether extracellular ROS accumulation is responsible for lethal lung inflammation during coinfection, we evaluated the efficacy of antibiotics in  $Nox2^{+/-}$  mosaic mice. Indeed, although all groups of coinfecting mice displayed comparable declines in viral and bacterial burdens at 6 dpi (Fig. 9, A and B), attenuation of acute lung damage was detected only in  $Nox2^{-/-}$  but not mosaic females (Fig. 9, C–E). Likewise, the extracellular release of phagocyte myeloperoxidase (MPO) into airways significantly increased in WT and mosaic mice, although their overall lung MPO levels were comparable to those in  $Nox2^{-/-}$  animals (Fig. 9 F). Similar to WT controls but in sharp contrast to  $Nox2^{-/-}$  animals, mosaic mice succumbed to influenza and MRSA coinfection despite antibiotic treatments (Fig. 9, G and H). Together, these results suggest that Nox2-induced systemic oxidative stress is responsible for lethal lung damage during coinfection.

**Nox2 inhibitor in conjunction with antibiotic treatment protects against lethal influenza and MRSA coinfection**

To investigate the practical application of findings from Nox2-deficient mice, we evaluated the effect of the NADPH oxidase-specific inhibitor apocynin (Wang et al., 1994; Stefanska et al., 2012) in conjunction with antibiotics for treatment of influenza-complicated MRSA infection. Although statistically insignificant, initiating apocynin administration 24 h before MRSA superinfection, i.e., 6 d post-influenza infection, tended to improve animal survival ( $P = 0.15$ ), particularly at the later stage of coinfection (Fig. 10 A). Consistent with this finding, we observed significantly attenuated lung damage in apocynin-treated mice at 7 dpi (Fig. 10 B). Furthermore, we evaluated the therapeutic effect of apocynin by initiating the administration 24 h after MRSA superinfection. The proportion of necrotic cells tended ( $P = 0.059$ ) to decline in airway inflammatory cells from apocynin-treated mice (Fig. 10 C), even though there were comparable lung viral and bacterial burdens in apocynin- or PBS-treated mice at 3 dpi (unpublished data). However, likely because of the differential animal survival in these two groups by 6 dpi (unpublished data), we were unable to quantitatively demonstrate an attenuation of lung damage in apocynin-treated mice (Fig. 10 D). Nonetheless, at this later time point, all surviving mice exhibited effective control of virus and bacteria but not inflammatory lung damage (Fig. 10, D–G). Importantly, even though treatment with the inhibitor apocynin alone was not sufficient to improve protection (Fig. 10H–I), in conjunction with antibiotic treatment, apocynin significantly reduced the mortality rate of coinfecting mice (Fig. 10 J). Together, our results demonstrate that therapeutic administration of NADPH oxidase inhibitor and appropriate antibiotic can rescue mice from influenza and MRSA coinfection.

**DISCUSSION**

Our study establishes that oxidative burst is critically involved in the pathogenesis of influenza and MRSA coinfection. Compared with WT controls, Nox2-deficient mice exhib-

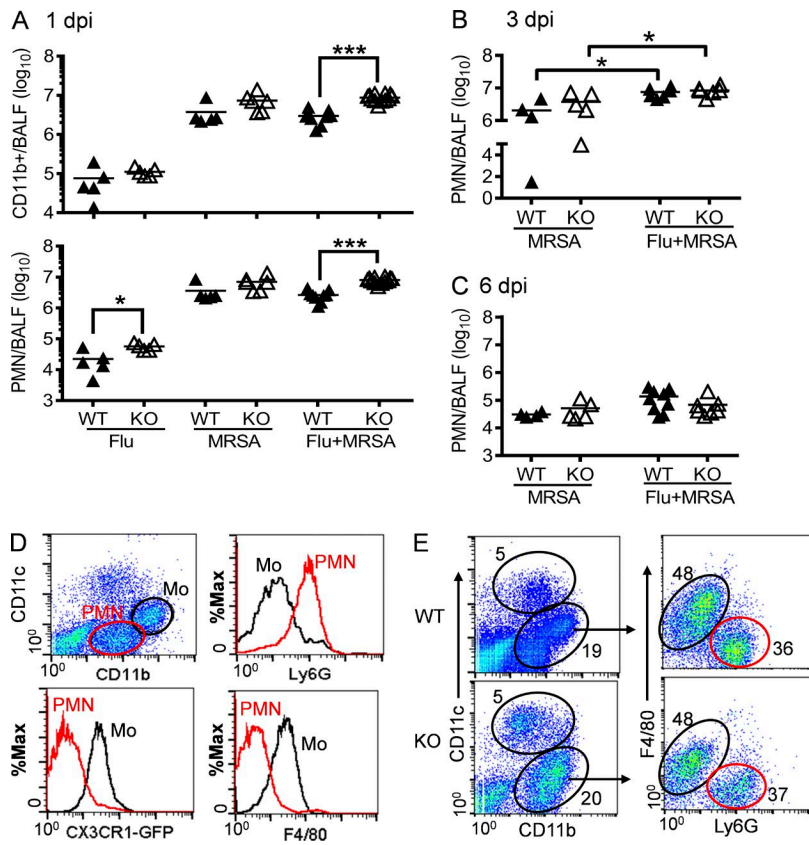


**Figure 6. Influenza and MRSA coinfection induces both inflammatory monocytes and neutrophils into airways.** (A–C) Mice were infected with PR8 and 7 d later superchallenged with MRSA. BALF cells from WT and Nox2-deficient (KO) mice were analyzed for numbers of CD11b<sup>+</sup> myeloid cells or neutrophils at days 1 (A), 3 (B), and 6 (C) post-infection. \*,  $P < 0.05$ ; \*\*\*,  $P < 0.001$ , Student's *t* test. (D) Flow cytometry analysis of airway inflammatory monocytes (Mo) and neutrophils (PMN) in coinfecting CX<sub>3</sub>CR1<sup>EGFP</sup> mice ( $n = 4$ ) at 6 dpi. (E) BALF cells from WT and Nox2-deficient (KO) mice were analyzed for the compositions of CD11b<sup>+</sup> myeloid cells (mean of five mice/group) at 6 dpi. All infected mice were treated daily with linezolid until 24 h before harvesting the samples. Data shown are representative of at least two independent experiments.

ited attenuated lung damage yet increased bacterial burdens after coinfection. In contrast, antibiotic treatment rescued Nox2-deficient mice but failed to protect fully WT animals, indicating Nox2 as a primary source of lethal lung injury. Thus, the reported high mortality rate from influenza and *S. aureus* coinfection, even with appropriate antibiotic treatment, appears attributable to Nox2-induced inflammatory tissue damage. Importantly, we found that antibiotic treatment in conjunction with an NADPH oxidase inhibitor significantly improved survival from post-influenza MRSA infection.

Secondary bacterial infection after influenza is known to cause severe pneumonia (Metersky et al., 2012). Compromised immune defense against either influenza virus or bacteria is suggested to contribute to disease pathogenesis (Sun and Metzger, 2008; Small et al., 2010; Iverson et al., 2011; Kudva et al., 2011). In particular, multiple mechanisms are reported to be involved in influenza-induced susceptibility to subsequent *S. aureus* infection (Small et al., 2010; Kudva et al., 2011; Robinson et al., 2013; Sun and Metzger, 2014). These previous studies described an association between suppression of innate immunity and consequent defects in bacterial control after influenza infection. However, how these innate immune responses lead to the disparate outcomes of suppressed antibacterial immunity but exaggerated lung inflammation remains unclear. Indeed, to our knowledge, no previous studies directly address the contribution of inflammatory damage to the pathogenesis of *S. aureus* pneumonia apart from defective antibacterial immunity.

In our influenza–MRSA coinfection model, bacterial infection was controlled through daily administration of antibiotics commonly used in MRSA patients, including linezolid, gentamicin, and vancomycin. The majority of antibiotic-treated WT mice still died from coinfection, even though the MRSA strain used in the study was sensitive to these antibiotics, as indicated in the Mouse model of viral and bacterial infection section of Materials and methods. As such, our lethal coinfection model replicates the poor outcome of patients with post-influenza *S. aureus* infection despite appropriate antibiotic treatment (Metersky et al., 2012). Importantly, this unique approach allowed us to investigate coinfection pathogenesis independent of defective bacterial killing.

Excessive lung inflammation is a key feature of clinical influenza and/or bacterial pneumonia. For example, a coinfection model of influenza and *Legionella* by Jamieson et al. (2013) showed that the lethal disease outcome resulted from impaired ability to tolerate tissue damage, rather than defective bacterial control. In agreement with Jamieson, Liu et al. (2013) showed that antibiotic therapy alone did not prevent the maximal weight loss of influenza and *S. aureus*-coinfecting mice. Conversely, Ghoneim and McCullers (2014) found that the antiinflammatory agent corticosteroid rescued ampicillin-treated mice from severe secondary pneumococcal pneumonia. However, adjuvant corticosteroid did not prevent the development of severe influenza-complicated pneumonia, such as in adults during the 2009 H1N1 influenza

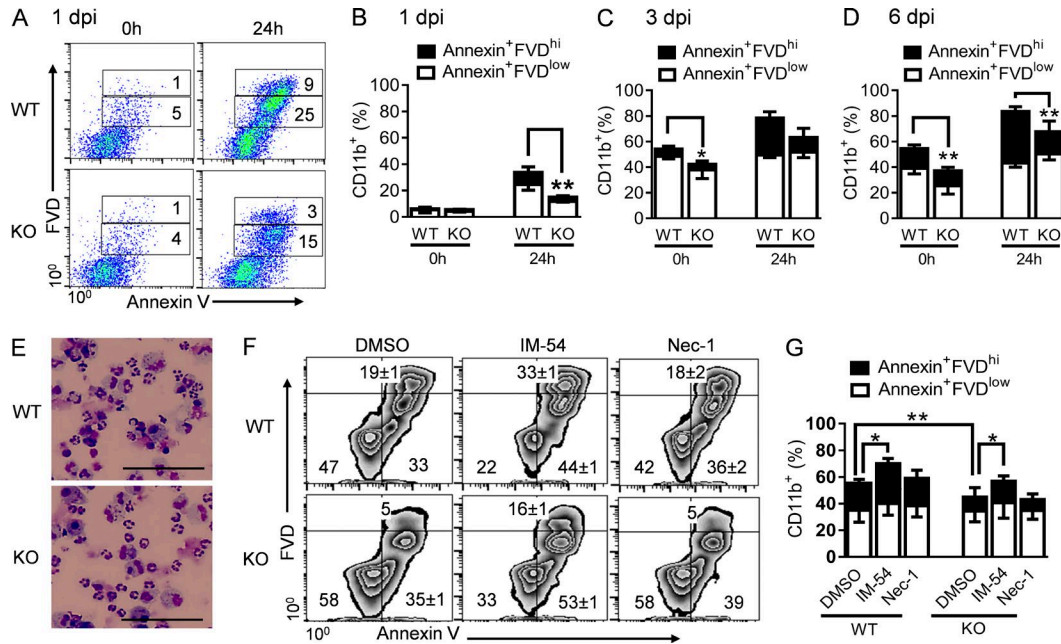


**Figure 7. Nox2 activity during coinfection reduces inflammatory cell survival.** (A–G) WT and Nox2-deficient (KO) mice were infected with PR8 and 7 d later superchallenged with MRSA. (A–D) CD11b<sup>+</sup> BALF cells ( $n = 4–5$ ) were analyzed by flow cytometry after staining with annexin V and FVD at the time of isolation (0 h), as well as 24 h after *in vitro* culture. \*,  $P < 0.05$ ; \*\*,  $P < 0.01$ , Student's *t* test. (A) Numbers indicate the mean percentages of four mice/group. (E) Diff-Quick-stained BALF cells from day 3 coinfecting WT and Nox2-deficient (KO) mice and after 24 h in culture. Bars, 50  $\mu$ m. (F and G) At 3 dpi, CD11b<sup>+</sup> BALF cells were stained with annexin V and FVD after 24 h in culture with IM-54, necrostatin 1 (Nec-1), or solvent control (DMSO). (F) BALF cells pooled from at least three mice per group are shown (mean  $\pm$  SD of triplicate wells). \*,  $P < 0.05$ ; \*\*,  $P < 0.01$ , paired Student's *t* test. All coinfecting mice were treated daily with linezolid (A–D) or gentamicin (E–G) until 24 h before harvesting the samples. Data shown in (A–F) are representative of at least two independent experiments. Data shown in G were combined from four independent experiments. Error bars represent SD.

pandemic (Kim et al., 2011; Viasus et al., 2011). Notably, despite improved supportive care, there is currently no specific treatment for inflammatory lung damage that is based on a known molecular pathway.

Nox2 activation in phagocytes is required for immune defense against numerous microbial pathogens, including *S. aureus* (Sun and Metzger, 2014). Even in circumstances in which oxidative burst is dispensable for microbial killing, Nox2 can attenuate or aggravate inflammation through fundamentally different mechanisms. In humans, defects in X chromosome-linked Nox2 can lead to CGD, and CGD patients suffer from a variety of inflammatory conditions, presumably because of defective neutrophil apoptosis (Deresinski, 2014). In mouse models, during pulmonary infection of fungal *Coccidioides*, Nox2 limits neutrophil infiltration to attenuate lung inflammation (Gonzalez et al., 2011). Moreover, after intratracheal challenge with zymosan or lipopolysaccharide, Nox2 reduces inflammatory cytokine production and thus facilitates resolution of lung inflammation (Segal et al., 2010). Interestingly, during pneumococcal pneumonia, although Nox2 deficiency facilitates neutrophil infiltration, it is not associated with lung injury. Instead, in this case, Nox2 deficiency facilitates bacterial clearance and thereby improves disease outcome.

During infection with H3N2 subtype influenza virus X31, Nox2 not only inhibits early viral clearance (3 dpi), but

also promotes lung pathology (Snelgrove et al., 2006; Vlahos et al., 2011). Despite this, compared with X31-infected WT controls, Nox2-deficient females (*Nox2*<sup>-/-</sup>) were found to have increased airway accumulation of inflammatory cells and greater weight loss (Snelgrove et al., 2006); in contrast, X31-infected Nox2-deficient males (*Nox2*<sup>-/-</sup>) were reported to have decreased airway accumulation of macrophages but no difference in weight loss (Vlahos et al., 2011). Daily apocynin treatment, starting 3 d before X31 infection, enhanced early viral clearance (Vlahos et al., 2011). Nonetheless, none of these previous studies using Nox2-deficient mice or oxidase inhibitors has demonstrated a significant Nox2 effect on viral clearance, lung pathology, or animal mortality during infection with the highly virulent influenza virus PR8 (H1N1), which was used in the current study.

We have previously established that influenza infection suppresses Nox2-dependent bacterial clearance and enhances susceptibility to secondary MRSA infection (Sun and Metzger, 2014). In the current study, bacterial outgrowth is inhibited by antibiotic therapy, and conversely, we found that Nox2 activity exacerbates inflammatory lung damage. Collectively, these studies reveal a double-edged sword action of Nox2 activation during influenza–MRSA coinfection. However, rather than broadly decreased inflammatory responses, early IL-17 production and neutrophil recruitment in Nox2-defi-

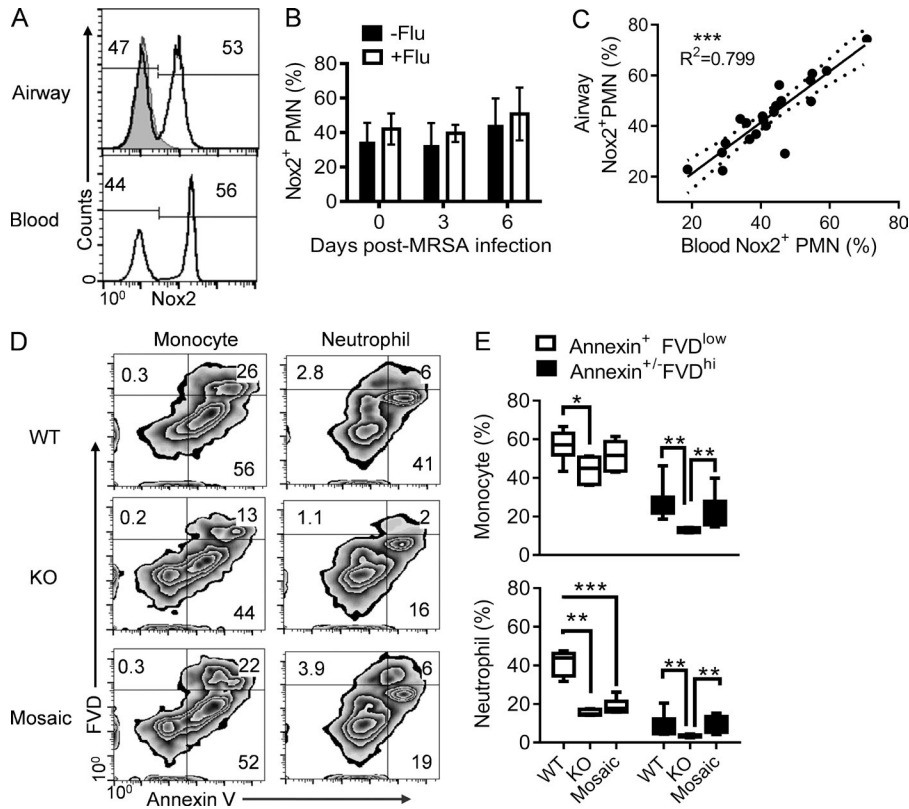


**Figure 8. *Nox2* activity accelerates necrotic cell death.** (A–E) Mice were inoculated with PR8 and 7 d later superchallenged with MRSA. (A–C) The percentages of *Nox2*-positive neutrophils in blood and airways at 6 dpi after coinfection (A), in blood (B), and in airways (C) at various days after MRSA or PBS inoculation of *Nox2*<sup>+/−</sup> mosaic mice (*n* = 5) with (+Flu) or without (−Flu) before PR8 infection. Mice were treated daily with linezolid until 24 h before harvesting the samples. (A) The gray histogram represents neutrophils in *Nox2*<sup>−/−</sup> airways. \*\*\*, *P* < 0.001, Pearson correlation. (D and E) Annexin V and FVD staining of inflammatory monocytes and neutrophils in WT (*n* = 8), *Nox2*<sup>−/−</sup> (KO; *n* = 5), and *Nox2*<sup>+/−</sup> (mosaic; *n* = 6) mice at 6 dpi. (D) Numbers indicate the mean percentages. Coinfected mice were treated daily with gentamicin until 24 h before harvesting the samples. \*, *P* < 0.05; \*\*, *P* < 0.01; \*\*\*, *P* < 0.001, Mann Whitney test. Data shown in B and C were combined from three independent experiments. Data shown in A, D, and E are representative of at least two independent experiments. Error bars represent SD.

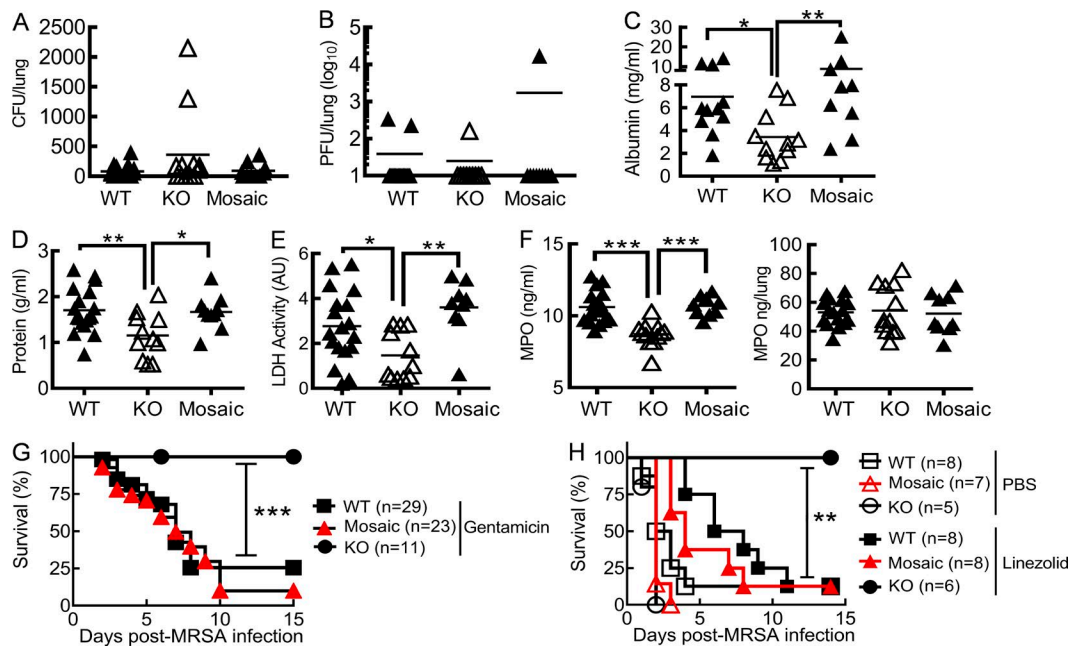


**Figure 9. Antibiotic therapy is insufficient to rescue *Nox2*<sup>+/−</sup> mosaic mice from coinfection.** (A–F) WT, *Nox2*<sup>−/−</sup> (KO), and *Nox2*<sup>+/−</sup> (Mosaic) females were infected with PR8 and 7 d later superchallenged with MRSA. At 6 dpi, lungs were analyzed for bacterial burdens (A), viral titers (B), albumin (C), protein (D), LDH activities (E), and MPO (F) in BALF. Coinfected mice were treated daily with gentamicin until 24 h before harvesting the samples. \*, *P* < 0.05; \*\*, *P* < 0.01; \*\*\*, *P* < 0.001, Mann Whitney test (C) or Tukey's multiple comparisons test (D–F). AU, arbitrary units. (G and H) Survival of WT, *Nox2*<sup>−/−</sup> (KO), and *Nox2*<sup>+/−</sup> (Mosaic) mice after superchallenge of day 7 PR8-infected mice with MRSA. \*\*, *P* < 0.01; \*\*\*, *P* < 0.001, log-rank test. Coinfected mice were treated daily with gentamicin (G), linezolid, or PBS (H). Data shown in A–G were combined from two independent experiments. Data shown in H are representative of two independent experiments.

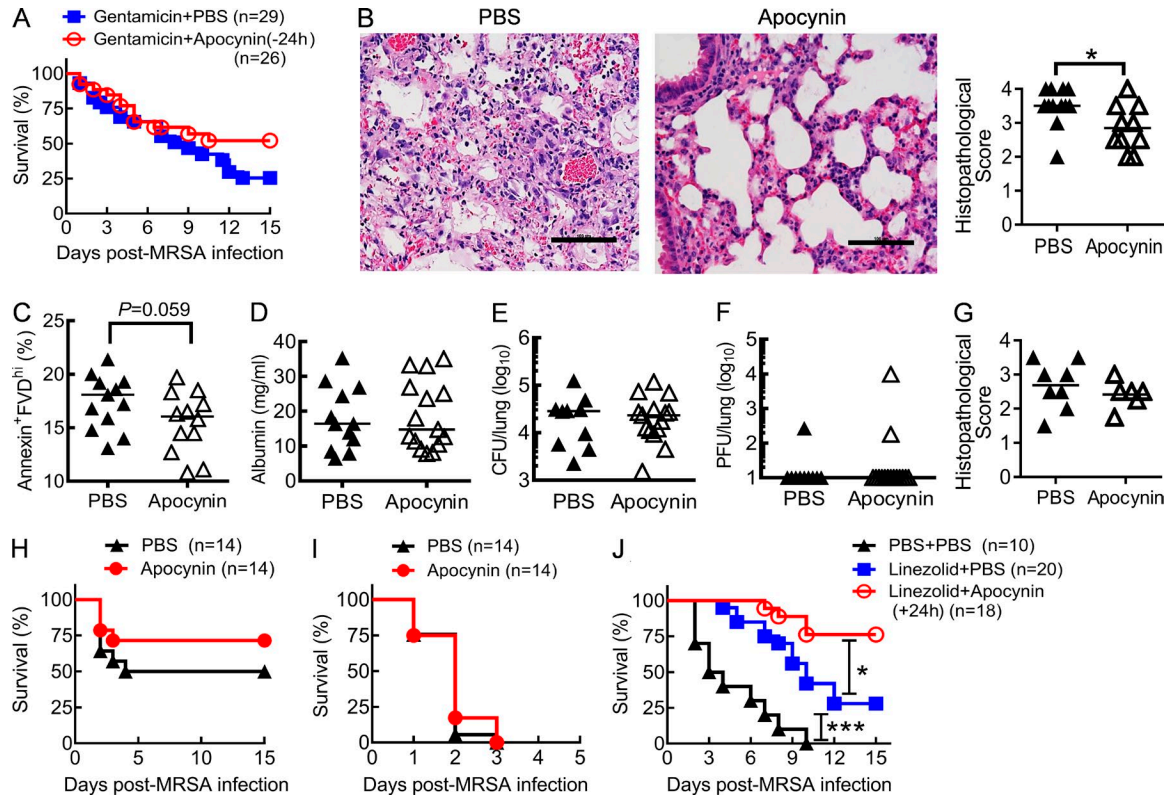


Figure 10. **Antibiotic treatment in conjunction with NADPH oxidase inhibitor improves protection against coinfection.** (A–J) Mice were inoculated with PR8 and 7 d later superchallenged with MRSA. (A and B) Survival (A) and day 7 lung histopathology (H&E; B) of coinfecting mice treated daily with apocynin (Gentamicin + Apocynin) or PBS (Gentamicin + PBS) beginning at 24 h before MRSA infection (–24 h). Bars, 100  $\mu$ m. \*,  $P < 0.05$ , Student's *t* test. (C) The percentages of annexin<sup>+</sup>FVD<sup>hi</sup> inflammatory cells (CD11b<sup>+</sup>) from day 3 coinfecting mice after 24 h in culture. (D–F) BALF albumin levels, bacterial burdens, and viral titers on day 6, and lung histopathology (G) on day 7 after coinfection. (C–G) Coinfecting mice were treated daily with apocynin or PBS beginning at 24 h after MRSA infection. All mice were treated daily with the antibiotics gentamicin (A–C and G) or linezolid (D–F) until 24 h before harvesting the samples. (H and I) Survival of PR8 and 0.25-mg (H) or 0.5-mg (I) MRSA coinfecting mice in the absence of antibiotic treatment. (J) Survival of PR8 and 0.5-mg MRSA coinfecting mice after treatments with PBS control (PBS + PBS), linezolid alone (Linezolid + PBS), or linezolid plus apocynin (Linezolid + Apocynin) beginning at 24 h after MRSA infection (+24 h). \*,  $P < 0.05$ ; \*\*\*,  $P < 0.001$ , log-rank test. Data shown are representative of two independent experiments (G) or were combined from two (H–J) or three (A–F) independent experiments.

cient mice instead increase during coinfection. Even so, this effect is transient, considering that neutrophil numbers dramatically decline in both WT and Nox2-deficient mice at the later stage of coinfection. Compared with the magnitude of inflammatory cell influx, inappropriate cell death is a more important source of acute lung injury (Bratton and Henson, 2011). In agreement, after influenza and *S. aureus* coinfection, we found that CD11b<sup>+</sup> inflammatory cells in WT airways exhibited a significant reduction in survival time.

The half-life of circulating and tissue-infiltrating neutrophils is generally regulated by apoptosis (Hofman, 2004). This programmed form of cell death and subsequent removal of apoptotic cells by macrophages is known to be critical for resolving inflammation (Bratton and Henson, 2011). However, it is also known that during inflammation, monocytes/macrophages are ineffective in apoptotic cell uptake (Jennings et al., 2005). In the absence of efferocytosis, excessive apoptotic cells will undergo autolytic secondary necrosis (do Vale et al.,

2007; Silva, 2010). Therefore, we speculate that the impact of Nox2-derived ROS on inflammatory lung damage is context dependent, i.e., when apoptotic cells can be promptly cleared, Nox2-induced cell death is antiinflammatory; in contrast, when apoptotic cells cannot be effectively cleared by efferocytosis, e.g., after influenza infection, Nox2 activity prompts secondary necrosis and subsequent inflammatory damage.

We show in this *in vivo* model that coinfecting mice exhibit substantial proinflammatory cytokine responses (Fig. 5) and thereby extensive airway neutrophil recruitment at 1 dpi (Fig. 6 A). Although neutrophil numbers remain elevated at 3 dpi, over half of the inflammatory cells were dying (Fig. 7 C), which in turn lead to 100-fold decreases in neutrophil numbers at 6 dpi (Fig. 6, B and C), coinciding with pronounced decreases in inflammatory cytokine production at these later stages of coinfection. Together, this indicates that during coinfection, the host immune response proceeds from an initial hyperinflammatory phase into a more extended immuno-

suppressive phase, similar to that observed in septic patients (Hotchkiss et al., 2013).

Considering the simultaneous recruitment, death, and removal of inflammatory cells at different phases of coinfection, we recognized the limitations of our *in vivo* model for detailed cellular and molecular analysis of Nox2-driven inflammatory cell death. Instead, we examined the possible effect of pharmacological inhibitors on inflammatory cell death *ex vivo*. IM-54 is a selective inhibitor of necrosis but not apoptosis (Sodeoka and Dodo, 2010), whereas necrostatin 1 is an inhibitor of necroptosis, i.e., an apoptosis-independent mode of programmed cell death (Su et al., 2015). However, neither IM-54 nor necrostatin 1 inhibited necrotic death of inflammatory cells isolated from coinfecting mice. Therefore, we propose that rather than oxidative stress-induced direct necrosis or necroptosis, secondary necrosis after apoptosis is the prevailing form of inflammatory cell death. Nonetheless, these pharmacological inhibitors are generally used for examining death pathways of tissue cells, so their regulatory effects on oxidative stress-induced necrotic cell death are probably cell type and context dependent. As such, in our *ex vivo* model, IM-54 actually accelerates inflammatory cell death (Fig. 7 G).

We have previously shown that *Nox2*<sup>+/-</sup> mosaic mice, similar to *Nox2*<sup>-/-</sup> females, are susceptible to post-influenza MRSA infection in the absence of antibiotic treatment (Sun and Metzger, 2014). However, in contrast to *Nox2*<sup>-/-</sup> females, antibiotic treatment failed to attenuate lung damage and reduce mortality in mosaic mice. Furthermore, mosaic mice showed significant increases in the percentage of necrotic inflammatory cells. Together, these data suggest that Nox2-induced systemic oxidative stress is responsible for accelerated necrotic cell death and lethal lung damage during coinfection. Conversely, the proportion of apoptotic neutrophils is reduced in mosaic mice. We speculate that this reduction is a combined result of increased survival of Nox2-deficient neutrophils and oxidative stress-accelerated secondary necrosis. Interestingly, the ratio of WT and Nox2-deficient neutrophils remains generally the same in mosaic mice before or after coinfection. These observations suggest that the overall impact of Nox2-derived ROS on the lifespan of circulating neutrophils is not cell intrinsic, even in the absence of influenza and/or MRSA infection.

Interestingly, our recent studies show that intracellular ROS in alveolar macrophages and neutrophils are in fact decreased at the recovery stage of influenza infection (Sun and Metzger, 2014). This negative regulation of oxidative burst has likely evolved to minimize lung damage during viral infection. Although intracellular ROS are reduced on a per cell basis during coinfection, there are excessive numbers of inflammatory cells, including both influenza-induced monocytes and *S. aureus*-induced neutrophils (Sun and Metzger, 2014). These inflammatory cells, in turn, release oxidants and other toxic molecules to airways. This event eventually culminates in lethal damage to surrounding lung tissue during coinfection.

Given that Nox2 is the catalytic subunit of NADPH oxidase in phagocytes, we focused the investigation on the regulatory effects of oxidative burst on myeloid cell death. We show that compared with influenza infection alone, MRSA superinfection induces extensive neutrophil infiltration (Fig. 6 A), and presumably, Nox2 activity in this phagocyte population is an important source of oxidative stress. In contrast, compared with MRSA infection alone, influenza infection specifically induces CCR2-dependent influx of inflammatory monocytes (Lin et al., 2011; Sun and Metzger, 2014). Moreover, despite their increased susceptibility to influenza infection alone (Aldridge et al., 2009), our ongoing studies revealed that CCR2-deficient mice are more resistant to influenza-MRSA coinfection, suggesting a detrimental role of airway monocytes during coinfection (unpublished data); however, future experimental evidence is needed to establish whether this adverse contribution of inflammatory monocytes to coinfection outcome is relevant to their Nox2 activity. Clinically, epithelial and endothelial injury is likely the ultimate cause of end-stage organ failure during ARDS or sepsis. Even though we cannot exclude the possibility that uncontrolled production of ROS can cause direct injury to lung epithelium at the later stage of infections, the findings in our studies suggest that Nox2 activity is the primary source of systemic oxidative stress during influenza-complicated MRSA coinfection.

In summary, our results demonstrate that influenza infection disrupts the delicate balance between Nox2-dependent antibacterial immunity and inflammation. This disruption leads to not only increased susceptibility to *S. aureus* infection, but also extensive lung damage. Importantly, we show that a combination treatment with antibiotics and a NADPH oxidase inhibitor significantly improved animal survival from coinfection. These findings suggest that treatment strategies that target both bacteria and oxidative stress will significantly benefit patients with influenza-complicated *S. aureus* pneumonia.

## MATERIALS AND METHODS

### Mouse model of viral and bacterial infection

Specific pathogen-free, C57BL/6 WT, *p47<sup>phox</sup>*<sup>-/-</sup> *Nox2*<sup>-/-</sup>, *Nox2*<sup>-/-</sup>, and CX3CR1<sup>EGFP</sup> mice were purchased from the Jackson Laboratory and bred at Albany Medical College and University of Nebraska Medical Center following Institutional Animal Care and Use Committee guidelines. C57BL/6 *Nox2*<sup>+/-</sup> (WT) males were mated with *Nox2*<sup>-/-</sup> females to produce *Nox2*<sup>+/-</sup> mosaic mice for the experiments. All animal experiments were approved by Albany Medical College Animal Care and Use Committee and University of Nebraska Medical Center, and all experiments were performed in accordance with Albany Medical College and University of Nebraska Medical Center Assurance of Compliance with Public Health Service Policy on Humane Care and Use of Laboratory Animals, which is on file with the Office of Protection from Research Risks, National Institutes of Health.

Viral challenge was performed with a sublethal (0.25 LD<sub>50</sub>), i.e., 25 PFU/female and 50 PFU/male, dose of PR8 administered i.n. to anesthetized, sex- and age-matched adult mice in 50  $\mu$ l of sterile PBS. Titers of virus stocks and viral levels in the bronchoalveolar lavage (BAL) fluids (BALFs) and lungs of infected mice were determined by plaque assays on Madin-Darby canine kidney cell monolayers. Bacterial coinfection was performed 7 d later (Sun and Metzger, 2014). To induce bacterial pneumonia, anesthetized mice were inoculated i.n. with 50  $\mu$ l PBS containing 0.25 mg (in Fig. 10 F) or 0.5 mg ( $\sim 2\text{--}6 \times 10^8$  CFU/mouse) of ATCC MRSA strain BAA-1695 (a *pvl*-isolate from patient sputum). Minimum inhibitory concentration values of antibiotics for MRSA BAA-1695 were  $\leq 12.5$   $\mu$ g/ml for gentamicin,  $\leq 1.17$   $\mu$ g/ml for vancomycin, and  $\leq 2.5$   $\mu$ g/ml for linezolid in vitro. Bacterial burden in the lungs was measured by sacrificing infected mice at the indicated time points and plating serial 10-fold dilutions of each sample onto blood agar plates.

### BAL cell analysis

BALF samples were collected by making an incision in the trachea and lavaging the lung twice with 0.8 ml PBS, pH 7.4. Total leukocyte counts were determined using a Bright-Line hemacytometer (Hausser Scientific).

For in vitro culture, BALF cells were washed and resuspended in DMEM supplemented with 10% FBS.  $1 \times 10^6$  BALF cells were added to the wells of a 96-well low-attachment plate (Costar) in presence of 10  $\mu$ g/ml IM-54 or 50  $\mu$ M necrostatin 1 for 24 h at 37°C. After overnight incubation, BALF cells were evaluated using Diff-Quick-stained cytospin preparations or flow cytometric analysis.

For flow cytometric analysis, BALF cells were incubated with 2.4G2 mAb against Fc $\gamma$ RII/III and stained with APC-conjugated anti-CD11c (BD), FITC-conjugated anti-CD11b (BD), PE-conjugated anti-Ly6G mAb (clone 1A8; BD), and APC-Cy7-conjugated anti-F4/80 (eBioscience) for myeloid cell analysis. Furthermore, APC-conjugated anti-CD11c (BD), PE-conjugated anti-CD11b (BD), PE-Cy7-conjugated anti-Ly6G mAb (BD), and APC-Cy7-conjugated anti-F4/80 (eBioscience) were used for myeloid cell analysis in CX3CR1<sup>EGFP</sup> mice. To differentiate early-stage apoptotic cells from the late-stage apoptotic and necrotic cells, BALF cells were stained with FVD eFluor 780 and annexin V PerCP-eFluor 710 (eBioscience), using FITC-conjugated anti-CD11b (BD), PE-conjugated anti-ly6G (BD), BV421-conjugated anti-F4/80 (BioLegend), and APC-conjugated anti-CD11c (BD) for cell surface markers. The stained cells were analyzed on a FACSCanto cell analyzer (BD) or LSRII-green flow cytometer (BD) using FACSDiva (BD) and FlowJo (Tree Star) software analysis.

**Detection of WT and Nox2-deficient neutrophils.** Nox2 expression in neutrophils was assessed with an anti-mouse gp-91phox mAb (BD; Sun and Metzger, 2014). In brief, after

staining for neutrophils with FITC-conjugated anti-mouse Ly6G mAb and PE-Cy7-conjugated anti-mouse CD11b mAb, cells were fixed and permeabilized before incubation with purified mouse anti-gp91phox mAb. Cells were then washed and incubated with PE-conjugated rat anti-mouse IgG1 Ab (BD) before analysis by flow cytometry.

### Determination of cytokine/chemokine production by ELISA.

BALF and lung homogenates were harvested and assayed for TNF, IL-1 $\beta$ , IL-6, IL-17, keratinocyte-derived chemokine, and MIP-2 by ELISA using commercially available kits from BD and R&D Systems.

**Lung histology analysis.** Mice were sacrificed 6 d after MRSA superinfection, and the lungs were removed for histological analyses. Paraffin-embedded tissues were sectioned to a thickness of 5  $\mu$ m and stained with hematoxylin and eosin (H&E) by standard methods.

**Evaluation of airway damage.** BALFs were harvested and assayed for albumin by ELISA using a commercially available kit from Bethyl Laboratories, Inc. MPO levels in BALF and lung homogenates were determined by ELISA (R&D Systems). Total protein levels and LDH activities in BALF were analyzed by a micro-bicinchoninic acid assay protein assay kit (Thermo Fisher Scientific) and an LDH cytotoxicity assay kit (Thermo Fisher Scientific), respectively.

### Treatment with antibiotics

Mice were i.p. injected with a therapeutic dose (100 mg/kg) of gentamicin at 3 h after MRSA infection and then followed by 50 mg/kg/d (Espersen et al., 1994). In some experiments, mice were treated s.c. with 50 mg/kg/d linezolid (Pfizer Inc.) or 150 mg/kg/d vancomycin beginning 2 h after MRSA infection (Reyes et al., 2011; Niska et al., 2013; Schuch et al., 2014). Control mice received PBS. All antibiotic treatment and sham injections continued through day 10 after MRSA infection.

### Treatment with apocynin

Mice were treated i.p. daily with 0.15 mg of apocynin (Sigma-Aldrich; Vlahos et al., 2011; Ferreira et al., 2013) in 100  $\mu$ l PBS initiated 24 h before or after and continued through day 10 after MRSA infection.

### Statistics

Results are expressed as means  $\pm$  SD. Significant differences between experimental groups were determined using a two-tailed Student *t* test (to compare two samples), an ANOVA analysis followed by Tukey's multiple comparisons test (to compare multiple samples), or a Mann Whitney test (non-parametric test) in Prism 6 (GraphPad Software). Survival analyses were performed using the log-rank test. For all analyses, a *p*-value  $< 0.05$  was considered to be significant.

## ACKNOWLEDGMENTS

The authors thank Melody Montgomery at the University of Nebraska Medical Center (UNMC) Office of the Vice Chancellor for Research Research Editorial Office for the professional editing of this manuscript. The authors also thank Dr. Philip Hexley and the UNMC Flow Cytometry Core Facility for assistance with FACS analysis, the UNMC Tissue Sciences Facility for staining and imaging tissue sections, and Dr. Kaihong Su for critical review of the manuscript.

This work was supported by a Pfizer Young Investigator award, a National Institutes of Health/National Heart, Lung, and Blood Institute grant (R01 HL118408) to K. Sun, and National Institutes of Health/National Institute of Allergy and Infectious Diseases grants (R01 AI75312) to D.W. Metzger.

The authors declare no competing financial interests.

Submitted: 19 March 2015

Accepted: 30 June 2016

## REFERENCES

- Abo, A., A. Boyhan, I. West, A.J. Thrasher, and A.W. Segal. 1992. Reconstitution of neutrophil NADPH oxidase activity in the cell-free system by four components: p67-phox, p47-phox, p21rac1, and cytochrome b-245. *J. Biol. Chem.* 267:16767–16770.
- Akaike, T., Y. Noguchi, S. Ijiri, K. Setoguchi, M. Suga, Y.M. Zheng, B. Dietzschold, and H. Maeda. 1996. Pathogenesis of influenza virus-induced pneumonia: involvement of both nitric oxide and oxygen radicals. *Proc. Natl. Acad. Sci. USA.* 93:2448–2453. <http://dx.doi.org/10.1073/pnas.93.6.2448>
- Aldridge, J.R. Jr., C.E. Moseley, D.A. Boltz, N.J. Negovetich, C. Reynolds, J. Franks, S.A. Brown, P.C. Doherty, R.G. Webster, and P.G. Thomas. 2009. TNF/iNOS-producing dendritic cells are the necessary evil of lethal influenza virus infection. *Proc. Natl. Acad. Sci. USA.* 106:5306–5311. <http://dx.doi.org/10.1073/pnas.0900655106>
- Blyth, C.C., S.A. Webb, J. Kok, D.E. Dwyer, S.J. van Hal, H. Foo, A.N. Ginn, A.M. Kesson, I. Seppelt, J.R. Iredell, ANZIC Influenza Investigators. COSI Microbiological Investigators. 2013. The impact of bacterial and viral co-infection in severe influenza. *Influenza Other Respi. Viruses.* 7:168–176. <http://dx.doi.org/10.1111/j.1750-2659.2012.00360.x>
- Bratton, D.L., and P.M. Henson. 2011. Neutrophil clearance: when the party is over, clean-up begins. *Trends Immunol.* 32:350–357. <http://dx.doi.org/10.1016/j.it.2011.04.009>
- Centers for Disease Control and Prevention (CDC). 2007. Severe methicillin-resistant *Staphylococcus aureus* community-acquired pneumonia associated with influenza—Louisiana and Georgia, December 2006–January 2007. *MMWR Morb. Mortal. Wkly. Rep.* 56:325–329.
- Deresinski, S. 2014. Chronic granulomatous disease: a potentially lethal combination of immunodeficiency and excess inflammation. *Clin. Infect. Dis.* 59:iii–iv.
- do Vale, A., C. Costa-Ramos, A. Silva, D.S. Silva, F. Gärtner, N.M. dos Santos, and M.T. Silva. 2007. Systemic macrophage and neutrophil destruction by secondary necrosis induced by a bacterial exotoxin in a Gram-negative septicemia. *Cell. Microbiol.* 9:988–1003. <http://dx.doi.org/10.1111/j.1462-5822.2006.00846.x>
- Espersen, F., N. Frimodt-Møller, L. Corneliussen, U. Riber, V.T. Rosdahl, and P. Skinhøj. 1994. Effect of treatment with methicillin and gentamicin in a new experimental mouse model of foreign body infection. *Antimicrob. Agents Chemother.* 38:2047–2053. <http://dx.doi.org/10.1128/AAC.38.9.2047>
- Ferreira, A.P., F.S. Rodrigues, I.D. Della-Pace, B.C. Mota, S.M. Oliveira, C.C. Velho Gewehr, F. Bobinski, C.V. de Oliveira, J.S. Brum, M.S. Oliveira, et al. 2013. The effect of NADPH-oxidase inhibitor apocynin on cognitive impairment induced by moderate lateral fluid percussion injury: role of inflammatory and oxidative brain damage. *Neurochem. Int.* 63:583–593. <http://dx.doi.org/10.1016/j.neuint.2013.09.012>
- Geering, B., and H.U. Simon. 2011. Peculiarities of cell death mechanisms in neutrophils. *Cell Death Differ.* 18:1457–1469. <http://dx.doi.org/10.1038/cdd.2011.75>
- Ghoneim, H.E., and J.A. McCullers. 2014. Adjunctive corticosteroid therapy improves lung immunopathology and survival during severe secondary pneumococcal pneumonia in mice. *J. Infect. Dis.* 209:1459–1468. <http://dx.doi.org/10.1093/infdis/jit653>
- Gonzalez, A., C.Y. Hung, and G.T. Cole. 2011. Absence of phagocyte NADPH oxidase 2 leads to severe inflammatory response in lungs of mice infected with *Coccidioides*. *Microb. Pathog.* 51:432–441. <http://dx.doi.org/10.1016/j.micpath.2011.08.003>
- Han, S., and R.K. Mallampalli. 2015. The acute respiratory distress syndrome: from mechanism to translation. *J. Immunol.* 194:855–860. <http://dx.doi.org/10.4049/jimmunol.1402513>
- Hofman, P. 2004. Molecular regulation of neutrophil apoptosis and potential targets for therapeutic strategy against the inflammatory process. *Curr. Drug Targets Inflamm. Allergy.* 3:1–9. <http://dx.doi.org/10.2174/1568010043483935>
- Hotchkiss, R.S., G. Monneret, and D. Payen. 2013. Sepsis-induced immunosuppression: from cellular dysfunctions to immunotherapy. *Nat. Rev. Immunol.* 13:862–874. <http://dx.doi.org/10.1038/nri3552>
- Imai, Y., K. Kuba, G.G. Neely, R. Yaghubian-Malhami, T. Perkmann, G. van Loo, M. Ermolaeva, R. Veldhuizen, Y.H. Leung, H. Wang, et al. 2008. Identification of oxidative stress and Toll-like receptor 4 signaling as a key pathway of acute lung injury. *Cell.* 133:235–249. <http://dx.doi.org/10.1016/j.cell.2008.02.043>
- Iverson, A.R., K.L. Boyd, J.L. McAuley, L.R. Plano, M.E. Hart, and J.A. McCullers. 2011. Influenza virus primes mice for pneumonia from *Staphylococcus aureus*. *J. Infect. Dis.* 203:880–888. <http://dx.doi.org/10.1093/infdis/jiq113>
- Jamieson, A.M., L. Pasman, S. Yu, P. Gamradt, R.J. Homer, T. Decker, and R. Medzhitov. 2013. Role of tissue protection in lethal respiratory viral-bacterial coinfection. *Science.* 340:1230–1234. <http://dx.doi.org/10.1126/science.1233632>
- Janssen, W.J., L. Barthel, A. Muldrow, R.E. Oberley-Deegan, M.T. Kearns, C. Jakubzick, and P.M. Henson. 2011. Fas determines differential fates of resident and recruited macrophages during resolution of acute lung injury. *Am. J. Respir. Crit. Care Med.* 184:547–560. <http://dx.doi.org/10.1164/rccm.201011-1891OC>
- Jennings, J.H., D.J. Linderman, B. Hu, J. Sonstein, and J.L. Curtis. 2005. Monocytes recruited to the lungs of mice during immune inflammation ingest apoptotic cells poorly. *Am. J. Respir. Cell Mol. Biol.* 32:108–117. <http://dx.doi.org/10.1165/rcmb.2004-0108OC>
- Kim, S.H., S.B. Hong, S.C. Yun, W.I. Choi, J.J. Ahn, Y.J. Lee, H.B. Lee, C.M. Lim, and Y. Koh. Korean Society of Critical Care Medicine H1N1 Collaborative. 2011. Corticosteroid treatment in critically ill patients with pandemic influenza A/H1N1 2009 infection: analytic strategy using propensity scores. *Am. J. Respir. Crit. Care Med.* 183:1207–1214. <http://dx.doi.org/10.1164/rccm.201101-0110OC>
- Kohanski, M.A., M.A. DePristo, and J.J. Collins. 2010. Sublethal antibiotic treatment leads to multidrug resistance via radical-induced mutagenesis. *Mol. Cell.* 37:311–320. <http://dx.doi.org/10.1016/j.molcel.2010.01.003>
- Köhler, J., K. Breitbach, C. Renner, A.K. Heitsch, A. Bast, N. van Rooijen, S. Vogelgesang, and I. Steinmetz. 2011. NADPH-oxidase but not inducible nitric oxide synthase contributes to resistance in a murine *Staphylococcus aureus* Newman pneumonia model. *Microbes Infect.* 13:914–922. <http://dx.doi.org/10.1016/j.micinf.2011.05.004>
- Kudva, A., E.V. Scheller, K.M. Robinson, C.R. Crowe, S.M. Choi, S.R. Slight, S.A. Khader, P.J. Dubin, R.I. Enelow, J.K. Kolls, and J.F. Alcorn. 2011. Influenza A inhibits Th17-mediated host defense against bacterial pneumonia in mice. *J. Immunol.* 186:1666–1674. <http://dx.doi.org/10.4049/jimmunol.1002194>

- Lin, K.L., S. Sweeney, B.D. Kang, E. Ramsburg, and M.D. Gunn. 2011. CCR2-antagonist prophylaxis reduces pulmonary immune pathology and markedly improves survival during influenza infection. *J. Immunol.* 186:508–515. <http://dx.doi.org/10.4049/jimmunol.1001002>
- Liu, Y., and J.A. Imlay. 2013. Cell death from antibiotics without the involvement of reactive oxygen species. *Science.* 339:1210–1213. <http://dx.doi.org/10.1126/science.1232751>
- Liu, X., Y. He, K. Xiao, J.R. White, D.N. Fusco, and G.A. Papanicolaou. 2013. Effect of linezolid on clinical severity and pulmonary cytokines in a murine model of influenza A and *Staphylococcus aureus* coinfection. *PLoS One.* 8:e57483. <http://dx.doi.org/10.1371/journal.pone.0057483>
- Louria, D.B., H.L. Blumenfeld, J.T. Ellis, E.D. Kilbourne, and D.E. Rogers. 1959. Studies on influenza in the pandemic of 1957–1958. II. Pulmonary complications of influenza. *J. Clin. Invest.* 38:213–265. <http://dx.doi.org/10.1172/JCI103791>
- Matute-Bello, G., C.W. Frevert, and T.R. Martin. 2008. Animal models of acute lung injury. *Am. J. Physiol. Lung Cell. Mol. Physiol.* 295:L379–L399. <http://dx.doi.org/10.1152/ajplung.00010.2008>
- Metersky, M.L., R.G. Masterton, H. Lode, T.M. File Jr., and T. Babinchak. 2012. Epidemiology, microbiology, and treatment considerations for bacterial pneumonia complicating influenza. *Int. J. Infect. Dis.* 16:e321–e331. <http://dx.doi.org/10.1016/j.ijid.2012.01.003>
- Metzger, D.W., and K. Sun. 2013. Immune dysfunction and bacterial coinfections following influenza. *J. Immunol.* 191:2047–2052. <http://dx.doi.org/10.4049/jimmunol.1301152>
- Niska, J.A., J.H. Shahbazian, R.I. Ramos, K.P. Francis, N.M. Bernthal, and L.S. Miller. 2013. Vancomycin-rifampin combination therapy has enhanced efficacy against an experimental *Staphylococcus aureus* prosthetic joint infection. *Antimicrob. Agents Chemother.* 57:5080–5086. <http://dx.doi.org/10.1128/AAC.00702-13>
- Reyes, N., J.B. Aggen, and C.F. Kostrub. 2011. In vivo efficacy of the novel aminoglycoside ACHN-490 in murine infection models. *Antimicrob. Agents Chemother.* 55:1728–1733. <http://dx.doi.org/10.1128/AAC.00862-10>
- Robinson, K.M., S.M. Choi, K.J. McHugh, S. Mandalapu, R.I. Enelow, J.K. Kolls, and J.F. Alcorn. 2013. Influenza A exacerbates *Staphylococcus aureus* pneumonia by attenuating IL-1 $\beta$  production in mice. *J. Immunol.* 191:5153–5159. <http://dx.doi.org/10.4049/jimmunol.1301237>
- Schuch, R., H.M. Lee, B.C. Schneider, K.L. Sauve, C. Law, B.K. Khan, J.A. Rotolo, Y. Horiuchi, D.E. Couto, A. Raz, et al. 2014. Combination therapy with lysin CF-301 and antibiotic is superior to antibiotic alone for treating methicillin-resistant *Staphylococcus aureus*-induced murine bacteremia. *J. Infect. Dis.* 209:1469–1478. <http://dx.doi.org/10.1093/infdis/jit637>
- Segal, B.H., W. Han, J.J. Bushey, M. Joo, Z. Bhatti, J. Feminella, C.G. Dennis, R.R. Vethanayagam, F.E. Yull, M. Capitano, et al. 2010. NADPH oxidase limits innate immune responses in the lungs in mice. *PLoS One.* 5:e9631. <http://dx.doi.org/10.1371/journal.pone.0009631>
- Short, K.R., E.J. Kroeze, R.A. Fouchier, and T. Kuiken. 2014. Pathogenesis of influenza-induced acute respiratory distress syndrome. *Lancet Infect. Dis.* 14:57–69. [http://dx.doi.org/10.1016/S1473-3099\(13\)70286-X](http://dx.doi.org/10.1016/S1473-3099(13)70286-X)
- Silva, M.T. 2010. Bacteria-induced phagocyte secondary necrosis as a pathogenicity mechanism. *J. Leukoc. Biol.* 88:885–896. <http://dx.doi.org/10.1189/jlhb.0410205>
- Small, C.L., C.R. Shaler, S. McCormick, M. Jeyanathan, D. Damjanovic, E.G. Brown, P. Arck, M. Jordana, C. Kaushic, A.A. Ashkar, and Z. Xing. 2010. Influenza infection leads to increased susceptibility to subsequent bacterial superinfection by impairing NK cell responses in the lung. *J. Immunol.* 184:2048–2056. <http://dx.doi.org/10.4049/jimmunol.0902772>
- Snelgrove, R.J., L. Edwards, A.J. Rae, and T. Hussell. 2006. An absence of reactive oxygen species improves the resolution of lung influenza infection. *Eur. J. Immunol.* 36:1364–1373. <http://dx.doi.org/10.1002/eji.200635977>
- Sodeoka, M., and K. Dodo. 2010. Development of selective inhibitors of necrosis. *Chem. Rec.* 10:308–314. <http://dx.doi.org/10.1002/trc.201000031>
- Stefńska, J., A. Sarniak, A. Włodarczyk, M. Sokolowska, E. Pniewska, Z. Doniec, D. Nowak, and R. Pawliczak. 2012. Apocynin reduces reactive oxygen species concentrations in exhaled breath condensate in asthmatics. *Exp. Lung Res.* 38:90–99. <http://dx.doi.org/10.3109/01902148.2011.649823>
- Su, X., H. Wang, D. Kang, J. Zhu, Q. Sun, T. Li, and K. Ding. 2015. Necrostatin-1 ameliorates intracerebral hemorrhage-induced brain injury in mice through inhibiting RIP1/RIP3 pathway. *Neurochem. Res.* 40:643–650. <http://dx.doi.org/10.1007/s11064-014-1510-0>
- Sun, K., and D.W. Metzger. 2008. Inhibition of pulmonary antibacterial defense by interferon- $\gamma$  during recovery from influenza infection. *Nat. Med.* 14:558–564. <http://dx.doi.org/10.1038/nm1765>
- Sun, K., and D.W. Metzger. 2014. Influenza infection suppresses NADPH oxidase-dependent phagocytic bacterial clearance and enhances susceptibility to secondary methicillin-resistant *Staphylococcus aureus* infection. *J. Immunol.* 192:3301–3307. <http://dx.doi.org/10.4049/jimmunol.1303049>
- Vardakas, K.Z., D.K. Matthaïou, and M.E. Falagas. 2009. Incidence, characteristics and outcomes of patients with severe community acquired-MRSA pneumonia. *Eur. Respir. J.* 34:1148–1158. <http://dx.doi.org/10.1183/09031936.00041009>
- Viasus, D., J.R. Paño-Pardo, E. Cordero, A. Campins, F. López-Medrano, A. Villoslada, M.C. Fariñas, A. Moreno, J. Rodríguez-Baño, J.A. Oteo, et al. Novel Influenza A (H1N1) Study Group, Spanish Network for Research in Infectious Diseases. 2011. Effect of immunomodulatory therapies in patients with pandemic influenza A (H1N1) 2009 complicated by pneumonia. *J. Infect.* 62:193–199. <http://dx.doi.org/10.1016/j.jinf.2011.01.014>
- Vlahos, R., J. Stambas, S. Bozinovski, B.R. Broughton, G.R. Drummond, and S. Selemidis. 2011. Inhibition of Nox2 oxidase activity ameliorates influenza A virus-induced lung inflammation. *PLoS Pathog.* 7:e1001271. <http://dx.doi.org/10.1371/journal.ppat.1001271>
- von Dessauer, B., J. Bongain, V. Molina, J. Quilodran, R. Castillo, and R. Rodrigo. 2011. Oxidative stress as a novel target in pediatric sepsis management. *J. Crit. Care.* 26:103e1–103e7.
- Wang, W., Y. Suzuki, T. Tanigaki, D.R. Rank, and T.A. Raffin. 1994. Effect of the NADPH oxidase inhibitor apocynin on septic lung injury in guinea pigs. *Am. J. Respir. Crit. Care Med.* 150:1449–1452. <http://dx.doi.org/10.1164/ajrccm.150.5.7952574>